

In-orbit Calibration and Validation of HY-2B Altimeter Using an Improved Transponder

Caiyun Wang, Mingsen Lin, Chaofei Ma, Ke Xu, Peng Liu, Te Wang, Bo Mu, Jinbiao Zhu, Wei Guo

Abstract—HY-2B (Haiyang) is the follow-on mission to HY-2A, the Chinese first sea satellite for oceanography, launched in Oct 2018. The main payloads onboard are similar to HY-2A. For the altimeter, an in-orbit calibration mode was designed to achieve higher calibration precision. An improved transponder was built and deployed for the calibration campaign. The purpose of the paper is to describe the in-orbit calibration and validation of HY-2B altimeter based on an improved transponder. A signal-rebuilt transponder was developed and employed in HY-2A altimeter calibration. It played an important role in quantitative analysis of HY-2A altimeter data products. For HY-2B altimeter, a newly-designed calibration mode was added, and an improved transponder was built. It has some advantages over the previous one in the rebuilt signal forms and modulation ways. Two calibration campaigns were carried out, in April 2019 and October 2020 at different sites. In the two campaigns, the precision of the altimeter range calibration is obtained less than 1 cm. For further validation and assessment to the result, a comparison between HY-2B and Jason-3 was performed in term of SSH (Sea Surface Height) on the tens of cross track points in the open ocean. The comparison result shows high degree of accuracy and stability of HY-2B altimeter instrument. In China's next five-year plan (2021-2025), many more transponders and related calibration facilities would be installed in the ocean calibration fields, serving a variety of different satellite altimetry missions.

Index Terms—HY-2B altimeter, in-orbit calibration, validation, improved transponder, integration.

I. INTRODUCTION

HY-2B is the second China's satellite for oceanic dynamic, launched in Oct, 2018. The main payloads on HY-2B, similar to HY-2A, include a dual-frequency radar altimeter, a three-band nadir-looking radiometer for atmospheric correction, and a Ku-band radar scatterometer [1].

HY-2A has been working for over 7 years. Some evaluations show the precision of SSH (Sea Surface Height) is more than 4 cm [2]-[4]. In HY-2B, a rubidium atomic clock is firstly used as the frequency reference to synchronize the USO (Ultra Stable Oscillator), therefore, the design accuracy of SSH for HY-2B is improved to 2 cm [1].

To provide truly global sea level within a geodetic system, also to obtain the altimeter instrument delay after launch, an

in-orbit calibration is essential. A signal-rebuilt transponder was employed in HY-2A altimeter calibration [5], [6]. The range calibration precision of better than 2 cm was obtained, and the HY-2A USO clock drift was also estimated accurately from the calibration data [7]-[9].

In order to have a thorough test and comprehensive verification prior to its launch, a fully functional return signal simulator (RSS) was developed in our lab [10], [11]. It can provide flexible echo forms, precise time delay, and better Signal to Noise Ratio (SNR), being an ideal simulator for the altimeter function test before its launch. Based on the RSS, an improved transponder was developed early in 2019, and employed in two calibration campaigns, April 2019 and October 2020, at different sites [12],[13].

Utilizing the CRS1 calibration facilities in West Crete, Greece, HY-2A altimeter SSH was assessed and compared with Jason series, SARAL/AltiKa, CryoSat-2, Sentinel-3, et al [20],[21]. The main facilities at CRS1 are offshore GPS buoys and coastal tide gauges, which provide a direct or an extrapolated SSH in-situ. The sea surface facilities are conventional methods used in calibration campaigns for many types of altimeters, which operate in a Low Resolution Mode (LRM), Synthetic Aperture Radar (SAR) mode or Interferometric Synthetic Aperture Radar (In-SAR) mode [14]-[25]. In recent years, inland lakes are also used for altimeter bias calibration, such as the Lake Issykkul in Kyrgyzstan for Jason-3 and Sentinel-3A [26].

Contrary to the sea surface facilities, the microwave transponder enables direct range measurements on land, and eliminates many error sources induced by the sea surface dynamics. The existing ground-based transponders, are bent-pipe ones, used in Jason-2, ERS-1/2, ENVISAT, Sentinel-3, Cryosat-2 for altimeter range bias calibration [27]-[31],[34]-[38] and backscatter coefficient sigma naught calibration [32],[33]. Bent-pipe transponder receives the altimeter signals, amplifies them and transmits them back to the altimeter. They are simple, economical, and stable, installed at a fixed location on the satellite ground tracks, providing a constant signal delay [34], [35].

A signal-rebuilt transponder was developed and employed in HY-2A altimeter calibration, which is different from the bend-pipe ones. The bend-pipe transponder is simple and stable, but it provides constant time delay introduced by the electronic devices in the transponder [30]. Therefore the bend-pipe transponder could be used only on a fixed position, waiting for the satellite passing over. On the contrary, the signal-rebuilt transponder can capture, track altimeter pulses, and transmit the rebuilt signals to the altimeter [5]. It is rather flexible, utilized in different positions on a mobile platform. The arrival time of the altimeter pulses at the transponder could be estimated accurately by the de-chirping technique [6]. Jitters on the rising edges of the rebuilt signals are rather small by using an atomic clock in the transponder, and the inaccuracies introduced from them could be decreased greatly by

Caiyun Wang, Ke Xu, Peng Liu, Te Wang, Wei Guo are with the National Space Science Center, Chinese Academy of Sciences, Beijing, 100190, China (e-mail: wangcaiyun@mirslab.cn; xuke@mirslab.cn; liupeng@mirslab.cn; wangte@mirslab.cn; guowei@mirslab.cn)

Mingsen Lin, Chaofei Ma, Bo Mu are with the National Satellite Ocean Application Service, Beijing, 100081, China (e-mail: mslin@mail.nsoas.org.cn; mcf@mail.nsoas.org.cn; mubo@mail.nsoas.org.cn)

Jinbiao Zhu is with the Aerospace Information Research Institute, Chinese Academy of Sciences, Beijing, 100094, China (e-mail: 10663548@qq.com)

Corresponding author: Mingsen Lin (e-mail: mslin@mail.nsoas.org.cn)

averaging multiple rebuilt pulses. The rebuilt signals are not identical to the received ones. The difference between them could be eliminated from the captured pulses, in which the frequency difference between the altimeter pulses and the transponder local oscillator could be estimated accurately and compensated in the rebuilt signals.

For HY-2B, an improved transponder was designed and utilized in two calibration campaigns. The altimeter instrument delay is obtained, and the range calibration precision is better than 1cm [12].

II. IMPROVEMENT AND CHARACTERIZATION OF HY-2B ALTIMETER TRANSPONDER

A. Improvements over the Previous Transponder

A newly-designed calibration mode was added to HY-2B altimeter, in which the raw I/Q data of all the odd number pulses in one burst was downloaded. Compared with HY-2A, only one pulse obtained every four bursts, the available data is greatly increased.

Based on the signal-rebuilt transponder for HY-2A and the RSS [10], [11], some improvements were done in the new built transponder, including digital Intermediate frequency (IF), Direct Digital Synthesis (DDS), time-division frequency modulation, self-calibration, etc.

B. Characters and Performance of the Improved Transponder

The transponder captures and tracks altimeter pulses, records them, and transmits the rebuilt signals to the altimeter [5]. It provides flexible time delay and many forms of rebuilt signals. Furthermore, as a result of the capture and tracking feature, the altimeter clock drift could be derived from the calibration data [6]. The working principle is shown in Fig.1.

HY-2B transponder consists of three main sub-units: antenna, Radio Frequency (RF) unit and digital control unit. The altimeter RF pulses are received by the transponder, de-chirped, and the narrowband Intermediate frequency (IF) signals are obtained, which are then sampled and demodulated to digital In-Phase and Quadrature (I/Q) signals. The advantage of the digital method is to achieve high phase orthogonality and amplitude consistency. After modulation and digital analog (D/A) conversion, the rebuilt signals are output to the RF transmitter.

The real transponder is shown in Fig.2. It is carried in a truck. During experiments, the antenna is set up on a tripod, and the other electronic devices are fixed in the truck. Some auxiliary instruments are necessary. A set of static Global Navigation Satellite System (GNSS) is needed to obtain the transponder accurate geographic location and the atmospheric delay at zenith. A laser rangefinder is used to relate the GPS antenna to the transponder antenna phase center. A portable power is charged each time before experiments to supply for all the electronic devices. A portable computer (PC) is needed for parameter input, data download and monitoring during the satellite passing over. The main specifications of HY-2B transponder are tabulated in Table I.

C. Sub-units of the Transponder

A broad band circular-polarization low side-lobe parabolic reflector antenna is employed, installed on a tripod during experiments. Its electrical performances are tested in a

chamber, shown in Fig.3. The results are listed in Table II.

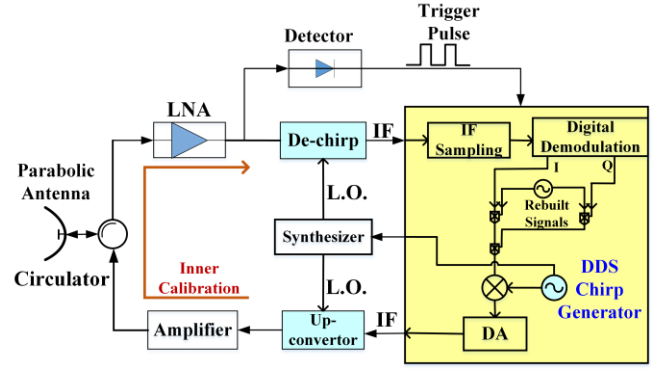


Fig.1. Block diagram of HY-2B improved transponder



Fig.2. Transponder for HY-2B altimeter in calibration

Table I HY-2B Transponder Specifications

Specification	Value
Center Frequency	13.58 GHz/5.25 GHz
Received Signal Bandwidth	320/80/20 MHz
Rebuilt Signal Bandwidth	320 MHz
Transmit Power	≥ 1 W
Rebuilt Signal Form	Direct Digital Synthesis
Reference Clock	Rubidium Atomic Clock
Antenna	Parabolic Reflector
Polarization	Circular
Platform	Vehicle Carried
Altimetry Calibration Precision	Better than 1 cm



Fig.3. Antenna test in a chamber

Table II Antenna Electrical Performances

Specification	Value
Frequency Range	2-15 GHz
Gain	≥ 40 dB
First Side-lobe Level	≤ -16 dB
Polarization	Dual circular
Standing-wave Ratio (SWR)	1.25
Transmit-receive Isolation	≥ 85 dB
Cross Polarization Isolation	≥ 30 dB
Pointing Precision	0.01°

The RF unit is an important part of the device, performing RF signal receiving, transmitting, down-conversion and frequency synthesis. It includes an RF front end, an RF receive/transmit module and a frequency synthesizer.

Two dependent channels, Ku and C band, are in the front end, illustrated in Fig.4. The received and transmitted signals are separated by a circulator. A coupler is utilized to test a portion of transmitted signals, performing the inner calibration of the transponder system. The inner calibration is performed each time before and after the satellite passing over, to monitor the variations of time delay and system gain of the transponder.

The RF receive module is to de-chirp the RF signals and down-convert them to IF. The two de-chirp Local Oscillators (L.O.) are at $12.48 \text{ GHz} \pm 160 \text{ MHz}$ and $4.15 \text{ GHz} \pm 160 \text{ MHz}$. A switch is used to share the IF channel, as illustrated in Fig.5. The narrowband 1.1 GHz IF signals are down-converted to 140 MHz, and output to the digital control unit.

The RF transmit module is to up-convert the rebuilt signals to RF pulses. The rebuilt signals are generated in the digital control unit, center frequency at 140 MHz. They are then up-converted to 1.1 GHz. The two transmit chirp L.O.s are $12.48 \text{ GHz} \pm 160 \text{ MHz}$ and $4.15 \text{ GHz} \pm 160 \text{ MHz}$, as illustrated in Fig.6. The RF pulses are then output to the RF front end, through the two circulators to the antenna.

A rubidium atomic clock is used in the synthesizer as the reference frequency source, to obtain high precision and stability. It generates all the required clock signals. The phase-lock loop (PLL) technology and frequency doubling and mixing technologies are used in the synthesizer.

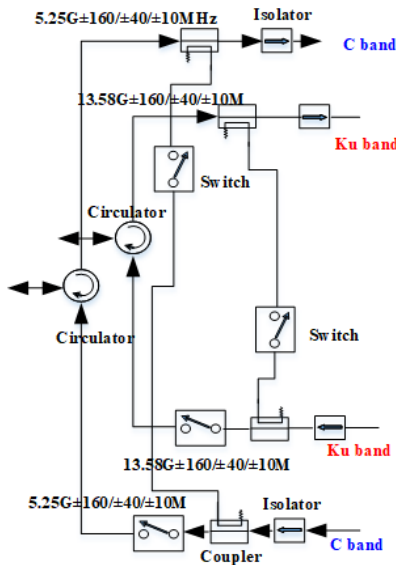


Fig.4. Block diagram of RF front end

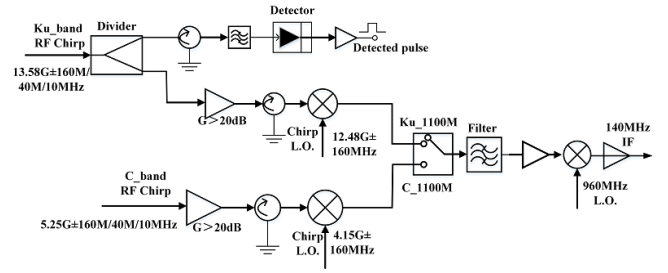


Fig.5. Block diagram of RF receive module

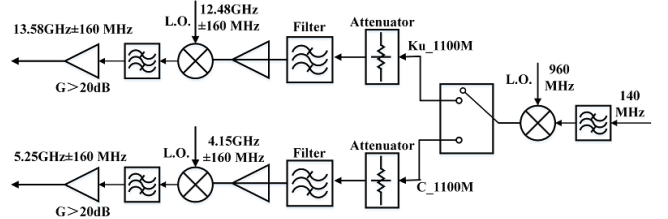


Fig.6. Block diagram of RF transmit module

The digital control unit is the kernel of the transponder, providing the system sequential logic control and signal processing.

In HY-2B transponder, the analog quadrature modulators are replaced by digital modulators based on Field Programmable Gate Array (FPGA), obtaining a better phase quadrature and amplitude balance of the baseband I/Q signals.

The IF 140 MHz signals are demodulated and recorded in FPGA. Then the rebuilt signals are generated and modulated in frequency or time to ensure the transmitted RF signals enter the altimeter receiving windows accurately. A DDS circuit is developed in the digital control unit to generate the required chirp L.O.s. Compared with the analog method, the DDS provides a variety of rebuilt signal forms, flexible time delay, better frequency linearity and low spurious. The DDS generated chirps are shown in Fig.7, by a modulation domain analyzer. They are negative frequency rate. The center frequency and bandwidth are 125 MHz and 40 MHz. Its pulse width is 102.4 μs . The DDS chirps are multiplied to $250 \text{ MHz} \pm 40 \text{ MHz}$, then are mixed with 2870 MHz and multiplied by four, and the $12.48 \text{ GHz} \pm 160 \text{ MHz}$ L.O. are obtained. These chirps are then mixed with 12030 MHz and 3700 MHz, and the $4.15 \text{ GHz} \pm 160 \text{ MHz}$ L.O. chirps are obtained, which is illustrated in Fig.8.

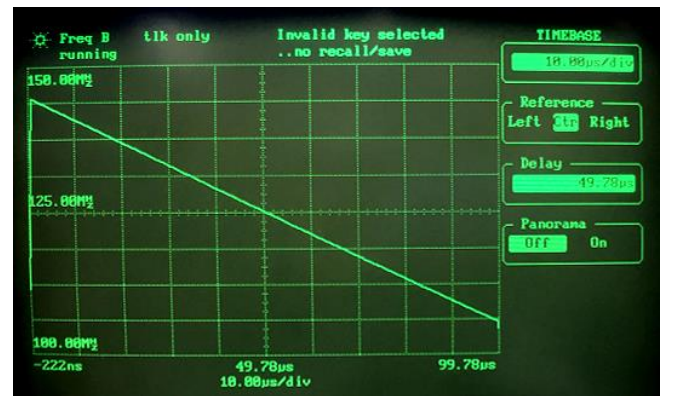


Fig.7. Frequency linearity of DDS chirp

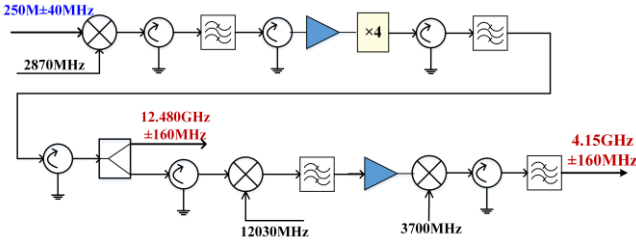


Fig.8. Block diagram of L.O. chirps

HY-2B altimeter receiving window is ± 60 meters. For the transponder transmitted signals to enter the windows, accurate orbit predication is essential. However, the short-term orbit prediction could have an error of dozens of meters to more than one hundred. To enable the transponder transmitted signals enter the altimeter window accurately. A time-division frequency modulation technique is used, equivalent to extending the altimeter receiving window. The rebuilt signals are divided into four time-equal segments, each modulated different frequencies. These are 0 MHz, 1.01 MHz, -0.17 MHz and -1.34 MHz, as displayed in Fig.9. Using this technique, the experiment success ratio is greatly improved.

As expected, the altimeter received echo signals are time-divided. There are two segments in the receiving window, segment one and three, shown in Fig.10. As the satellite passes, the other segments can enter the receiving window. Using this technique, the amount of the echo data is greatly increased. Therefore, the calibration precision, which heavily depends on the available echo data, is improved dramatically.

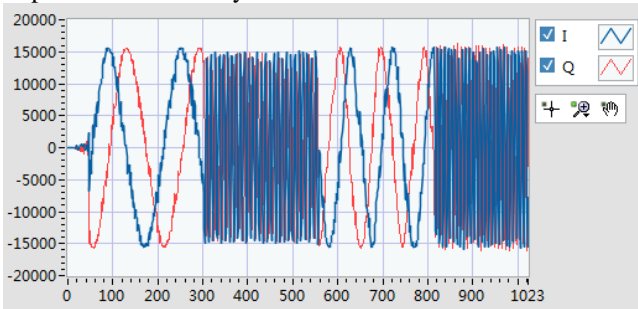


Fig.9. Time-division frequency modulated signals

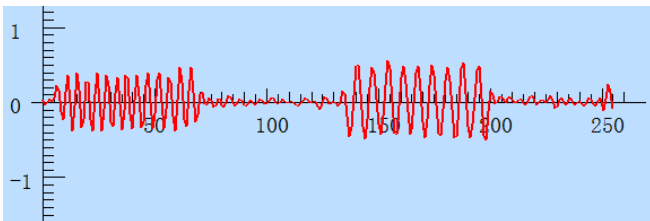


Fig.10. Segmented echo signals received on HY-2B

D. Integration Test and Self-calibration

The transponder integration and test were done in our lab, using a RSS [10]. The two instruments are connected by two low loss RF cables. The RSS transmits RF pulses at the same time sequence as HY-2B altimeter, which are captured, tracked, and recorded by the transponder. Then the transponder rebuilds pulses and transmits them back to the RSS. The transponder rebuilt signals displayed in a spectrum analyzer, as in Fig.11.

The transmitted Ku and C bands signals are 13.58 GHz±160MHz and 5.25 GHz±160 MHz, negative frequency rate. Its pulse width is 102.4 μ s. The maximum power is more than 30 dBm. The transmitted power is controlled by

the software installed on a portable PC. During in-orbit experiments, the output power is attenuated 10 dB - 20 dB to ensure the altimeter receiver safety.



Fig.11. Transponder rebuilt and transmitted signals spectrum

An entire system self-calibration is essential to acquire the transponder instrument delay. It was performed by using a reflector disk installed on a delicate two-dimension support, placed at a far distance from the transponder. The experiment was performed before the in-orbit calibration campaign, as shown in Fig.12.

The received echoes are shown in Fig.13, marked with a red circle. The spectrum index indicates the round distance from the transponder to the disk. The geometric distance between the transponder antenna and the disk is measured by a laser rangefinder. Subtract the geometric distance from the round, and the transponder instrument delay is obtained. Its instrument delay is 18.81 meters. The range reference point is at the end of the feed horn. During the self-calibration, an inner loop delay was recorded and was referred to as the in-orbit calibration reference. The delay of the transponder (D_TRP) measured in the Lab was used afterwards in the field calibration as the transponder instrument hardware delay. If there are some modifications to the transponder hardware, another self-calibration is necessary to obtain the new D_TRP.



Fig.12. Self-calibration of the transponder

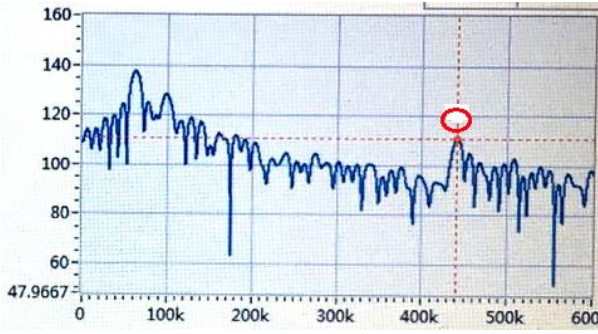


Fig.13. Echo spectrum in self-calibration (x-axis is number of FFT points, 4096 points implemented, y-axis represents relative power of signals)

III. IN-ORBIT CALIBRATION OF HY-2B ALTIMETER USING THE IMPROVED TRANSPONDER

A. Principle and Methods of Calibration

The aim of the in-orbit calibration is to obtain the altimeter system delay, including instrument delay and clock drift bias. The instrument delay depends on the altimeter hardware state after the satellite was launched, which is supposed to be relevant to the instrument aging. The clock drift bias is due to the USO drift. Both theses could be acquired accurately from the calibration data. The altimeter system delay could be expressed as:

$$d_{sys} = d_{alt} + d_{USO} \quad (1)$$

$$= (d_{range} - d_{wet} - d_{dry} - d_{iono} - d_{tide} - d_{TRP}) - d_{orbit}$$

d_{sys} is the altimeter system delay, d_{alt} is the instrument delay, d_{USO} is the clock drift bias. d_{range} is the measured range to the transponder, including ionosphere delay, atmosphere delay, etc. d_{orbit} is the geometric distance from the satellite gravity center to the transponder phase center, as illustrated in Fig.14.

In formula (1), d_{TRP} is the transponder delay, including the instrument hardware delay 18.81 meters and the preset signal delay. The former's variations could be corrected by the inner calibration loop. The latter is a preset value calculated each time before the satellite passing over, according to the precise orbit prediction.

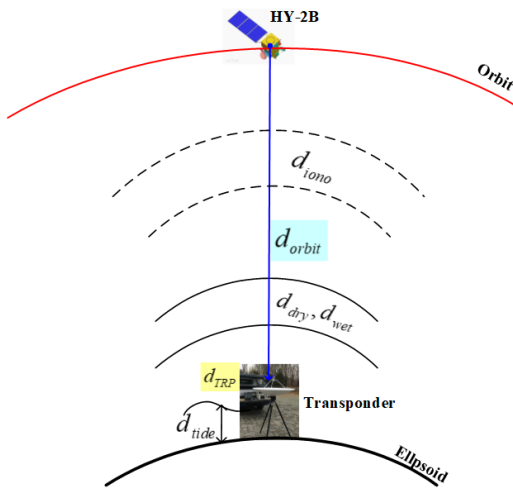


Fig.14. Geometric relationship between altimeter and transponder

The calibration precision could be evaluated by the standard deviation (std) of the d_{alt} , which is considered a

constant in a short period. Two experiment campaigns were carried out, from April to September 2019 and October 2020. The std of d_{alt} is obtained to be less than 1 cm in both of the two calibration campaigns. It shows that the HY-2B altimeter instrument is rather stable and the calibration results are reliable.

B. Selection of Calibration Sites

The orbit period of HY-2B is 14 days. To perform more calibration experiments in a shorter time, the transponder is designed mobile, carried on a truck.

The calibration sites were selected carefully to fulfill the following requirements:

- It should be under, or in the proximity of the ground tracks of HY-2B, within one kilometer;
- The echo from the transponder must be stronger and distinguishable from the surrounding returns;
- Location with high vegetation and buildings should be avoided;
- It should be easily accessible and have little personnel activities.

A reconnaissance survey took place in April 2019 and September 2020. In total ten sites were selected. All the sites are within 300 meters away from the ground tracks, being in open field, with low electromagnetic background. The locations are shown in Fig.15 and Fig.16, in south-east and south-central China.

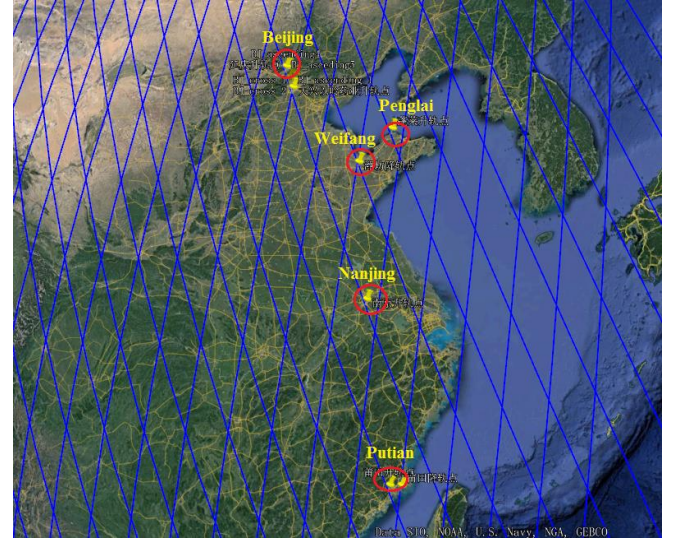


Fig.15. Calibration sites of HY-2B altimeter in 2019

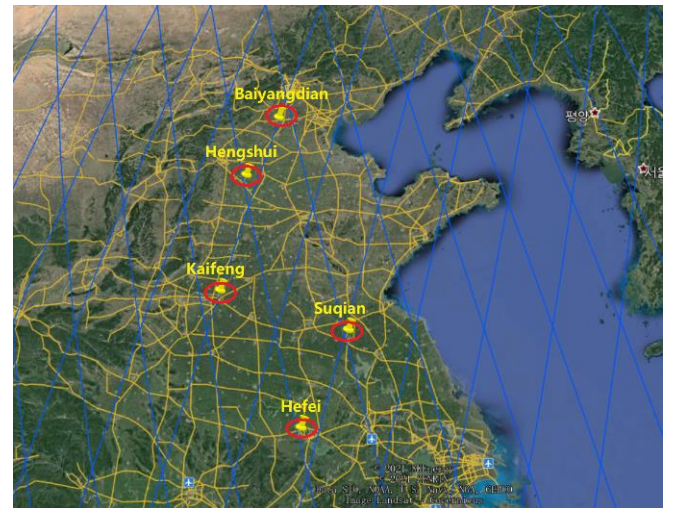


Fig.16. Calibration sites of HY-2B altimeter in 2020

The calibration sites are accurately positioned by a GNSS, listed in Table III.

Table III Precise Calibration Positions in South-east and South-central China (WGS-84 Coordinate Frame)

Site	Longitude (°)	Latitude (°)	Height (m)
Beijing	116.249194	39.815381	47.8698
Penglai	120.679023	37.776870	102.7370
Weifang	119.058578	36.739688	24.6891
Nanjing	118.813125	31.935415	11.2843
Putian	118.850447	25.314754	117.4341
Hengshui	115.000638	38.031333	31.5648
Kaifeng	114.196482	34.761298	60.1076
Suqian	118.189972	33.958163	21.9787
Heifei	117.013392	31.730535	51.9621

Except in Beijing, one experiment was performed in the other sites. HY-2B orbit period is approximately 14 days. The reasonable selection of the calibration sites is to perform as many experiments as possible. In each twenty days of calibration campaign, April 2019 and October 2020, nine and four experiments were done separately. It is much efficient than the fix-mode calibration, once in 14 days.

C. Procedure of in-orbit Calibration

For the accurate atmosphere correction and precise location determination of the transponder, a set of static GNSS is necessary. It was set up at least 8 hours prior to the satellite passing. The GNSS antenna should be in the vicinity of 10 meters to the transponder antenna.

Some preparation should be done including charging the battery, accurate orbit prediction and calculation of the transponder rebuilt signals delay. About 30 minutes before the satellite passing, the transponder antenna is set up on a sturdy tripod, which is two-dimensional adjusted in azimuth and pitch. A PC is used to monitor the transponder status and download the recorded data. When the satellite passes, the transponder tracks and altimeter signals, records them and rebuilds the RF signals to the altimeter. Two inner calibrations are done just a few minutes before and after the passing over, recording the variations of delay and gain of the transponder instrument. The entire procedure is performed automatically, controlled by the preset program in FPGA.

HY-2B orbit height is 970 kilometers. Its beam width is 1.1° [1], so the overhead time is about 2 - 3 seconds. After passing over, the antenna, the GPS as well as the battery etc., are collected and put in the truck. The procedure in one experiment is shown in Fig.17.

Because of the narrow bandwidth of HY-2B antenna and the transponder antenna, the accurate pointing between the two is crucial. HY-2B altimeter is nadir-looking. The transponder antenna must be pointing straight upwards. This is achieved by a high precision electronic level-meter. It is placed on the antenna feeder plane, which is perpendicular to the antenna electric axis by the mechanical technique. Its vertical error is less than 0.1° . The experimental scenario and antenna leveling adjustment are displayed in Fig.18 and Fig.19.

The geodetic height of the transponder antenna phase center is determined by the static GNSS, which height is referred to the bottom of the choke ring, and the transponder

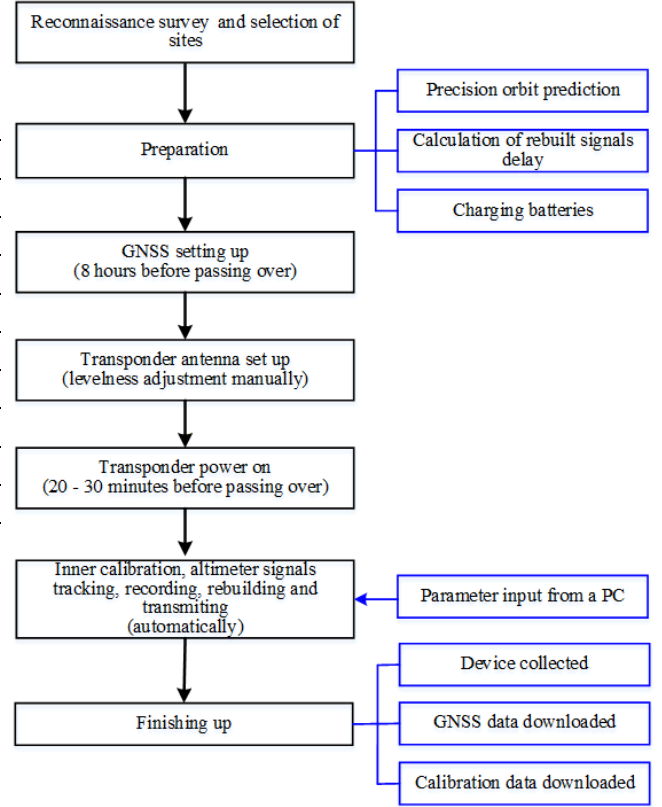


Fig.17. In-orbit calibration experiment procedure



Fig.18. HY-2B in-orbit calibration experiment scenario



Fig.19. Electronic level-meter used in experiment

height reference is at the feeder plane, therefor a laser level meter is utilized to correlate the GNSS geodetic height and

the transponder reference plane, as illustrated in Fig.20. The height difference X is measured accurately by a laser level meter in every experiment.

The GNSS antenna was set up at least 8 hours before the satellite passing. To acquire accurate position of the transponder, data from multiple GNSS fiducial stations as well as land state network are utilized, and the vertical precision of less than 1 cm could be obtained.

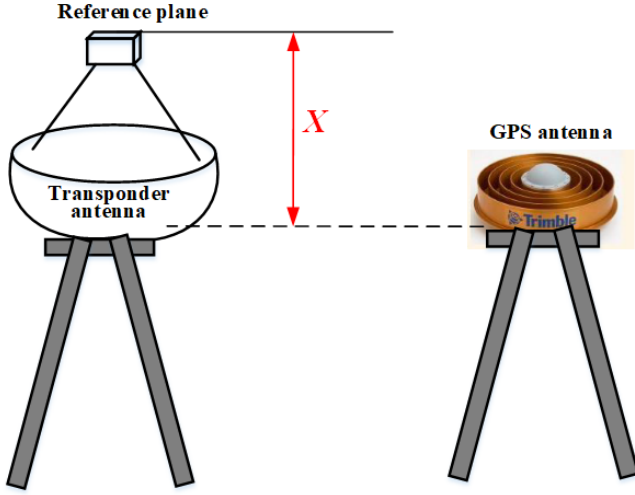


Fig.20. Transponder geodetic height determined by GNSS

D. Calibration data Processing and Key Techniques

A special calibration mode was designed on HY-2B, in which, the raw I/Q data of all the odd number pulses in one burst was downloaded, so the available calibration data is greatly increased. It is essential to improve the calibration precision. The downloaded data is indicated in Fig.21.

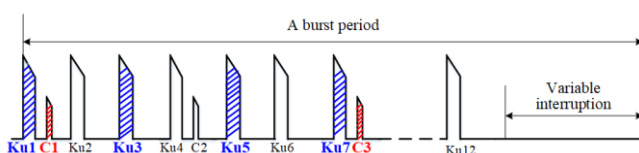


Fig.21. Indication of HY-2B downloaded odd number pulses in one period

Calibration data processing is complicated. It includes the following steps:

- The time-frequency domain conversion of the transponder data and the altimeter data;
- the accurate matching between the altimeter and the transponder pulses;
- obtaining the measured range from the altimeter data;
- obtaining the geometric distance from the precise orbit determination (POD) file and the GNSS data;
- correction to the measured range, including Doppler correction, propagation delay correction, transponder delay correction, tide correction, etc.;
- obtaining the altimeter system delay, including the clock drift bias and the instrument delay;
- subtracting the clock drift bias, obtaining the altimeter instrument delay;

The procedure is described in Fig.22.

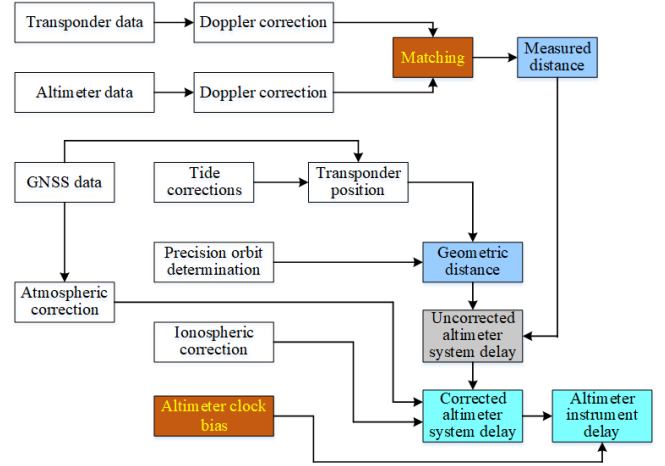


Fig.22. Flowchart of transponder calibration developed for HY-2B altimeter instrument delay estimation

The key techniques in the data processing are the altimeter-transponder pulse matching and the altimeter clock bias correction. The method to estimate HY-2B altimeter clock drift is similar to HY-2A [6], [7]. In HY-2B, a rubidium atomic clock is used [1]. It is rather stable, with very small long-term drift.

Establishing correspondence between altimeter data and transponder data is the first and crucial step in processing. A new method based on shape match of the Fast Fourier Transform (FFT) waveforms of the altimeter and transponder data is used. According the principle of the de-chirping, the transponder data is displayed in Fig.23. On the contrary, the altimeter data is as Fig.24. Their spectrums exhibit approximate mirror symmetry.

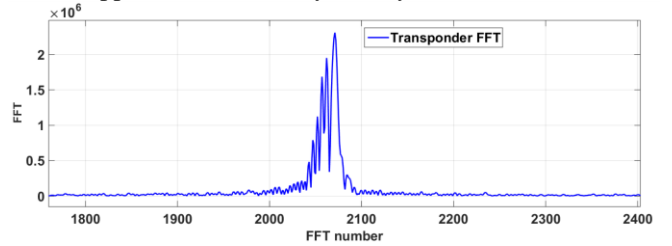


Fig.23. Transponder data FFT waveform (x-axis is number of FFT points, 4096 points implemented, y-axis represents relative power of signals)

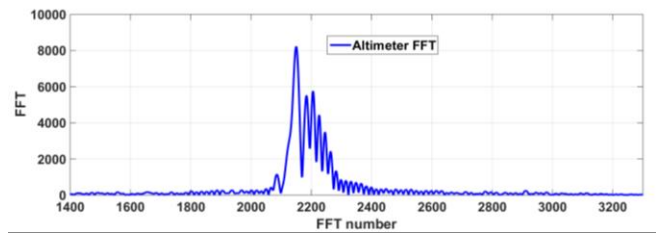


Fig.24. Altimeter data FFT waveform (x-axis is number of FFT points, 4096 points implemented, y-axis represents relative power of signals)

The abscissa of the maximum power in the FFT spectrum represents the time difference (or frequency difference) of the rising ends between the altimeter and the transponder pulses. In every successful experiment, about two or three hundreds of valid pulses are recorded and transferred in FFT. Therefore two sequences of frequency differences are obtained. For the frequency difference is included in the transponder rebuilt signals, the sequences of the altimeter and the transponder exhibit a similar shape, but in an opposite direction. Based on the shape characteristic matching, the corresponding relationship between the altimeter and the transponder would be established. The

matched forms of the two sequences are shown in Fig.25 and Fig.26. In Fig.26, there is a little amount of data missing because of tracking lost or spur noises, and the shape matching method is still valid in this case.

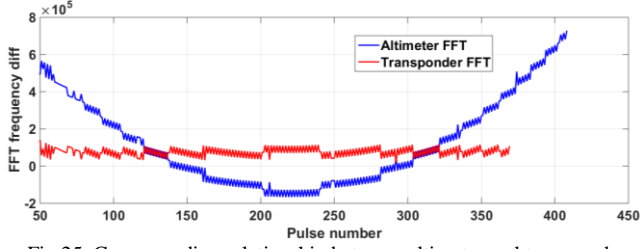


Fig.25. Corresponding relationship between altimeter and transponder (x-axis is recorded pulse number, y-axis represents FFT frequency difference)

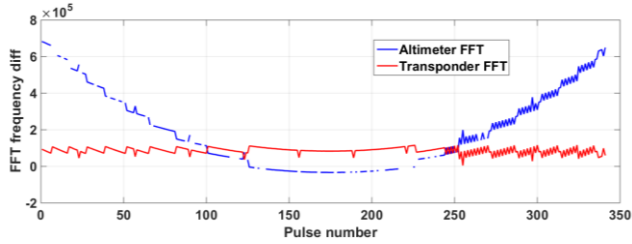


Fig.26. Corresponding relationship between altimeter and transponder with some data missing (x-axis is recorded pulse number, y-axis represents FFT frequency difference)

According to the relationship between the satellite-transponder geometric distance and the timing sequence of the pulses [29], [30], the point target response of the transponder moves all along the altimeter range window resulting in a typical parabolic signature, as shown in Fig.27. The blue curve presents the response of the transponder in the altimeter. The red one is the transponder measured one-way range changes relative to the closest approach. In the case of the clock synchronization of the satellite and the transponder, the vertexes of the two parabolas would coincidence. Therefore, according to the vertexes deviation, the clock bias between the satellite and the transponder could be acquired. The method of estimating the altimeter clock drift was described in [6], [7].

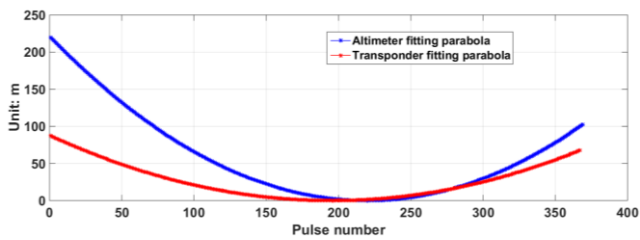


Fig.27. Parabola fitted from the raw transponder data and the altimeter data (x-axis is recorded pulse number, y-axis represents the pulse interval, converted to range, blue one is altimeter transmit-receive interval, red one is transponder receive-receive interval)

The POD file is obtained one day after the satellite passes over. It is a one-minute timescale file. To match the altimeter transmit-receive time sequence, a Hermite interpolation method is used. A sixteen-minute data is cut from the POD file, covering eight minutes before and after the overhead epoch. The interpolated geometric distance between the satellite and the transponder during the passing over is shown in Fig.28.

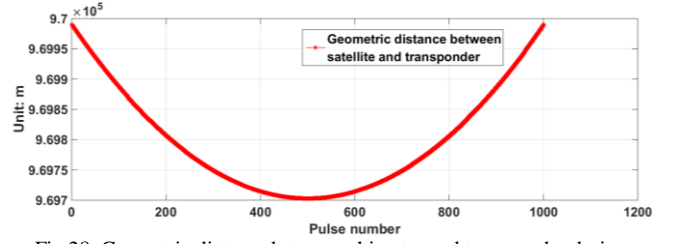


Fig.28. Geometric distance between altimeter and transponder during passing over (x-axis is recorded pulse number, y-axis represents the ranges)

IV. CALIBRATION RESULTS AND COMPARISON WITH JASON-3 ON CROSS TRACK POINTS

A. Calibration Results of HY-2B altimeter

The aim of the two calibration campaigns based on the improved transponder is to obtain HY-2B altimeter instrument delay and estimate its clock drift bias. The results show that the altimeter instrument is very stable. The on-board atomic clock is rather accurate. Its drift is almost negligible.

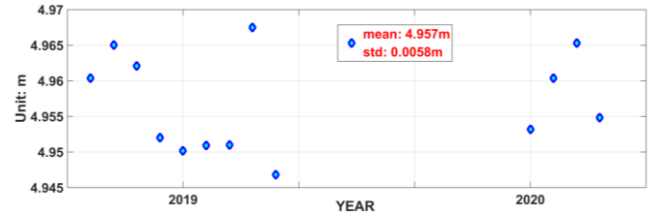


Fig.29. HY-2B altimeter instrument delay from in-orbit calibration experiments

In the two calibration campaigns April 2019 and October 2020, 13 successful experiments were done, 9 in 2019 and 4 in 2020. The mean of the altimeter instrument delay is 4.957 meters, and the standard deviation (std) is 0.68cm, shown in Fig.29.

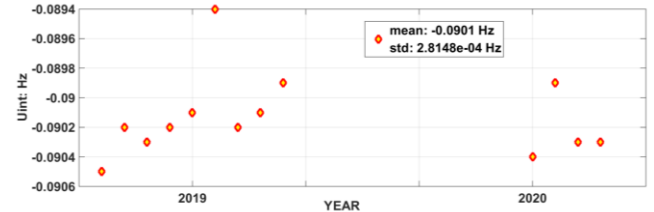


Fig.30. HY-2B altimeter clock drift bias from in-orbit calibration experiments

The clock drift is displayed in Fig.30. It presents a good stability in the two years of operation. The mean bias is less than 0.1 Hz. Its std is less than 0.001 Hz. The center frequency of the clock is 80 MHz. An important parameter is DF/F_0 where DF is the std deviation and F_0 is the center frequency. From the obtained results, the parameter DF/F_0 is less than 10^{-11} , which provides a best proof that HY-2B is much accurate and stable than HY-2A for the improvement of the clock from the oven controlled crystal oscillator (OCXO) to the rubidium atomic clock.

The range drift linked to the clock drift is shown in Fig.31. Its mean value is less than 0.5cm and the std is less than 10^{-3} cm, which means the range drift introduced by the clock drift is rather small.

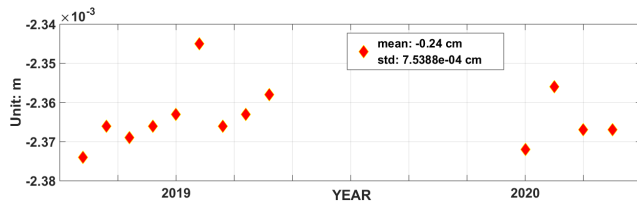


Fig.31. Range drift introduced by clock drift

B. Comparison with Jason-3 on Cross Track Points

HY-2B altimeter tracking bias to SSH is 14.508 meters. Its instrument delay is 4.957 meters. Therefore, the total correction of SSH is:

$$14.508 + 4.957 = 19.465 \text{ meters.}$$

For the further validation, the corrected SSH acquired from HY-2B Interim Geophysical Data Record (IGDR) data is compared with Jason3 at the cross track points in the open ocean on the Pacific and the Atlantic. The time window is 5 minutes and the distance window is 5 kilometers. The comparison results are shown in Fig.32. The mean of the SSH difference is 0.016 meters.

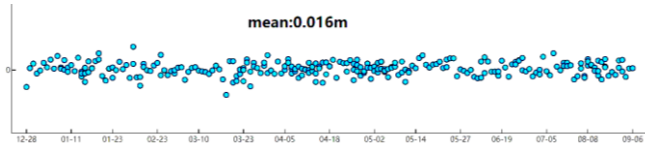


Fig.32. Comparison of SSH between HY-2B and Jason3 on cross track points from Dec 2019 to Sept 2020

The high degree of consistence on the cross track points provides a best validation that HY-2B altimeter measurements are accurate and stable, and the calibration method based on the improved transponder is reliable and effective.

V. CONCLUSION

An improved transponder was developed and employed in HY-2B altimeter in-orbit calibrations in 2019 and 2020. It offers a reliable and efficient approach to obtain the altimeter's instrument delay accurately. Furthermore, it provides a special method to monitor the long-term drift of the altimeter clock. The calibration and validation results show that HY-2B altimeter is rather stable and accurate in the SSH measurement. By utilizing a rubidium atomic clock, HY-2B clock drift is decreased significantly. It presents a good performance on long-term stability. In the following Haiyang series missions, HY-2C, launched in Oct 2020, and HY-2D, would be launched in May 2021, the transponders would be modified and improved further to meet the new calibration requirements and adapt to the different types of signals forms. With the construction of the Chinese first ocean calibration field in Wanshan islands, calibration infrastructure is under rapid development. In China's next five-year plan (2021-2025), many more transponders and related calibration facilities would be installed in the ocean calibration field, serving a variety of different satellite altimetry missions. With the infrastructure construction and the cooperation of multiple types of calibration devices, more accurate and a wider variety of calibration and validation achievements would be achieved.

ACKNOWLEDGEMENT

The author would like to thank the National Satellite Ocean Application Service for providing HY-2B Level 0 data and IGDR data, the HY-2B altimeter payload group for assistance in the development of the improved transponder and the in-orbit calibration campaigns.

REFERENCE

- [1] Ke Xu, Peng Liu, et al, "The improved design for HY-2B radar altimeter," in Proc. IGARSS 2017, Fort Worth Texas, USA, pp.534-537, Jul. 2017.
- [2] Maofei Jiang, Ke Xu, et al, "Range noise level estimation of HY-2B radar altimeter and its comparison with Jason-2 and Jason-3 altimeters," in Proc. IGARSS 2019, Yokohama, Japan, pp.8312 - 8315, Jul. 2019.
- [3] Maofei Jiang, Ke Xu, et al, "Evaluation of HY-2B altimeter products over ocean," in Proc. IGARSS 2020, Waikoloa, HI, USA, pp.5858- 5861, Sept-Oct. 2020.
- [4] Maofei Jiang, Ke Xu, et al, "Estimating the sea state bias of HY-2A radar altimeter by a three-dimensional nonparametric model," in Proc. IGARSS 2016, Beijing, China, pp.396- 399, Jul. 2016.
- [5] C. Y. Wang, W. Guo, F. Zhao and J. Zh. Wan, "In-orbit Calibration of HY-2A altimeter using a signal reconstructive transponder," in Proc. IGARSS 2014, Quebec, Canada, pp. 5119-5122, Jul. 2014
- [6] Caiyun Wang, Wei Guo, et al, "Development of the reconstructive transponder for in-orbit calibration of HY-2 altimeter[J]", IEEE JSTARS, Vol. 9, Issue.6, pp. 2709- 2719, Jun. 2016.
- [7] J. ZH. Wan, W. Guo, F. Zhao, C. Y. Wang, et al, "HY-2A radar altimeter ultrastable oscillator drift estimation using reconstructive transponder with its validation by multi-mission cross calibration," IEEE trans. Geosci. Remote Sens., vol.53, issue: 9, pp.5229-5236, Sept.2015.
- [8] J. ZH. Wan, W. Guo, F. Zhao, C. Y. Wang, et al, "Echo signal quality analysis during HY-2A radar altimeter calibration campaign using reconstructive transponder[J]", IEEE JSTARS, Vol. 9, Issue.6, pp. 2702-2708, Jun. 2016.
- [9] J. ZH. Wan, W. Guo, C. Y. Wang and F. Zhao, "A Matching Method for Establishing Correspondence Between Satellite Radar Altimeter Data and Transponder Data Generated During Calibration," IEEE Geosci. Remote Sens. Lett., vol.11, issue:12, pp. 2145-2149, Dec.2014.
- [10] Wei Guo, Caiyun Wang, et al, "Development and pre-launch test of a return signal simulator for HY-2B altimeter," in Proc. IGARSS 2018, Valencia, Spain, pp.1602 - 1605, Jul. 2018.
- [11] Caiyun Wang, Wei Guo, et al, "Development and performance analysis of a fully Functional return signal simulator for HY-2B scatterometer," in Proc. IGARSS 2018, Valencia, Spain, pp.9168 - 9171, Jul. 2018.
- [12] Caiyun Wang, Wei Guo, et al, "In-orbit calibration and validation of HY-2B altimeter using an improved transponder," in Proc. IGARSS 2020, Waikoloa, HI, USA, pp.5819- 5822, Sept-Oct. 2020.
- [13] Caiyun Wang, Wei Guo, et al, "Development and integration test of an improved transponder for HY-2B altimeter," in Proc. IGARSS 2020, Waikoloa, HI, USA, pp.5862- 5865, Sept-Oct. 2020.
- [14] M. Roca, R. Francis, et al, "RA-2 Absolute Range Calibration," Proc. of Envisat Validation Workshop, Frascati, Italy, 9-13 December 2002 (ESA SP-531, August 2003).
- [15] D.J. Wingham a, C.R. Francis, "CryoSat: A mission to determine the fluctuations in Earths land and marine ice fields," Advances in Space Research 37 (2006), pp.841-871, doi:10.1016/j.asr.2005.07.027.
- [16] S. P. Mertikas, A. Papadopoulos and Erricos C. Pavlis, "An alternative procedure for the estimation of the altimeter bias for the Jason-1 satellite using the dedicated calibration site at Gavdos," in Proc. SPIE, vol.7105, Remote Sensing of the Ocean, Sea Ice, and Large Water Regions 2008, 71050H, Oct.2008.
- [17] S. P. Mertikas, R. T. Ioannides, X. Frantzis, A. Tripolitsiotis, et al, "Recent developments for the estimation of the altimeter bias for the Jason-1&2 satellites using the dedicated calibration site at Gavdos," in Proc. SPIE, vol.7473, Remote Sensing of the Ocean, Sea Ice, and Large Water Regions, 74730C, Sept. 2009.
- [18] S. P. Mertikas, A. Daskalakis, V. Tserolas, W. Hausleitner, et al, "Absolute calibration of Jason satellite radar altimeters at Gavdos Cal/Val facility using independent techniques," in Proc. SPIE, vol.7825, Remote Sensing of the Ocean, Sea Ice, and Large Water Regions 2010, 78250C Oct.2010.
- [19] F. Frappart, N. Roussel, et al, "Preliminary result of the 2013 Ibiza calibration campaign of Jason2 and Saral altimeter," in Proc. IGARSS 2014, Quebec, Canada, pp. 4473-4476 Jul. 2014.
- [20] Stelios P. Mertikas, Xinghua Zhou, et al, "First preliminary results for the absolute calibration of the Chinese HY-2 altimetric mission using the

aCRS1 calibration facilities in West Crete, Greece,” *Advances in Space Research*, DOI: 10.1016/j.asr.2015.10.016, Available online, 17 Oct 2015, www.elsevier.com/locate/asr.

[21] Mertikas, S.P.; Donlon, C.; et al. “Gavdos/West Crete Cal/Val site: Over a decade calibrations for Jason series, SARAL/AltiKa, CryoSat-2, Sentinel-3 and HY-2 altimeter satellites,” In *Proceedings of the ESA Living Planet Symposium 2013 (ESA SP-740)*, Prague, Czech Republic, 9–13 May 2016.

[22] Phuong Lan Vu, Frédéric Frappart, “Multi-Satellite Altimeter Validation along the French Atlantic Coast in the Southern Bay of Biscay from ERS-2 to SARAL,” *Remote Sens.* 2018, 10, 93; doi:10.3390/rs10010093.

[23] Pascal Bonnefond, Olivier Laurain, et al. “Calibrating the SAR SSH of Sentinel-3A and CryoSat-2 over the Corsica Facilities,” *Remote Sens.* 2018, 10, 92; doi:10.3390/rs10010092.

[24] Jügang Yang, Jie Zhang, “Validation of Sentinel-3A/3B satellite altimetry wave heights with buoy and Jason-3 data,” *Sensors(Basel)*, v.19(13), 2019 Jul, DOI:10.3390/s19132914.

[25] Zhai Wanlin, Zhu Jianhua, et al, “Preliminary calibration results for Jason-3 and Sentinel-3 altimeters in the Wanshan Islands,” *Journal of Oceanology and Limnology*, Mar. 27, 2020, <https://doi.org/10.1007/s00343-020-9251-1>.

[26] Jean-François Créau, Muriel Bergé-Nguyen, Stéphane Calmant, et al, “Absolute Calibration or Validation of the Altimeters on the Sentinel-3A and the Jason-3 over Lake Issykkul (Kyrgyzstan),” *Remote Sensing*. 2018, 10, 1679; doi:10.3390/rs10111679.

[27] R. J. Powell, “Relative vertical positioning using ground-level transponders with the ERS-1 altimeter,” *IEEE Trans. Geoscience and Remote Sensing*, vol.GE24, no.3, pp.421-425, May. 1986.

[28] A. R. Birks, “Radar Altimeter Calibration Using Ground Based Transponders,” in *Proc. Envisat Symposium*, Montreux, Switzerland, ESA SP-636, pp.23 – 27, Apr.2000.

[29] Elena Cristea, Phil Moore, “Altimeter bias determination using two years of transponder observations,” in *Proc. ‘Envisat Symposium 2007’*, Montreux, Switzerland, pp. 23-27, Apr. 2007.

[30] W. Hausleitner, F. Moser, J.-D. Desjonqueres, F. Boy, N. Picot, J. Weingrill, S. Mertikas, “A new method of precise Jason-2 altimeter calibration using a microwave transponder,” *Marine Geodesy*, vol.35, no.1, pp. 337-362, Dec.2012.

[31]Albert Garcia-Mondejar, stelios Mertikas,et al, “Sentinel-3 Transponder Calibration Results,” 2017 Ocean Surface Topography Science Team Meeting, 23-27 October 2017 | Miami, USA.

[32] Pierdicca, N.; Bignami, C.; Roca, M.; Femenias, P.; Fascetti, M.; Mazzetta, M.; Loddo, C.N.; Martini, A.; Pinori, S. “Transponder Calibration of the Envisat RA-2 altimeter Ku band sigma naught,” *Adv. Space Res.* 2013, 51, 1478–1491.

[33]N. Pierdicca, C. Bignami, M. Fascetti, P. Femenias, et al, “Transponder calibration of the ENVISAT RA-2 altimeter sigma naught,” in *Proc. IGARSS 2012*, Munich, Germany, pp. 2675-2678, Jul.2012.

[34] S. P. Mertikas, Craig Donlon, et al, “Fifteen years of Cal/Val service to reference altimetry missions: calibration of satellite altimetry at the permanent facilities in Gavdos and Crete, Greece,” *Remote Sensing*. 2018, 10, 1557; doi:10.3390.

[35] Stelios Mertikas, Achilles Tripolitsiotis, et al, “A permanent infrastructure in Crete for the calibration of Sentinel-3, Cryosat-2 and Jason missions with transponder,” *Proc. ‘ESA Living Planet Symposium 2013’*, Edinburgh, UK, 9–13 September, 2013 (ESA SP-722, December 2013).

[36] Mertikas S. P., Craig Donlon, Pierre Féménias, et al, “Absolute calibration of the Sentinel-3 altimeter with sea-surface and transponder at FRM Standards in West Crete, Greece,” *International review workshop on satellite altimetry cal/val activities and applications*, 23-26 April 2018, Chania, Crete, Greece.

[37] Stelios Mertikas, Craig Donlon, et al, “Absolute calibration of the European Sentinel-3A surface topography mission over the permanent facility for altimetry calibration in west Crete Greece,” *Remote Sens.* 2018, 10, 1808; doi:10.3390/rs10111808.

[38] Stelios Mertikas, Achilleas Tripolitsiotis, et al, “The ESA permanent facility for altimetry calibration monitoring performance of radar altimeters for Sentinel-3A, Sentinel-3B and Jason-3 using transponder and sea-surface calibrations with FRM Standards,” *Remote Sens.* 2020, 12, 2642; doi:10.3390/rs12162642.

[39] M. B. Mathews, “Design, testing, and performance analysis of transponders for use with satellite altimeters,” Ph.D. dissertation, University of Colorado, Boulder, the USA, 1995.

[40] Ridha Touzi, R. K. Hawkins, and Stéphane Côté “High-Precision Assessment and Calibration of Polarimetric RADARSAT-2 SAR Using Transponder Measurements,” *IEEE trans. Geosci. Remote Sens.*, vol.51, No.1, pp.487-503, Jan.2013.



Wang Caiyun received the B.Eng. and M.Eng. degrees in communication and information engineering from Xidian University, Xi'an, China, in 1997 and 2001, respectively. She is an associate professor of the Nation Space Science Center, Chinese Academy of Sciences, Beijing. Her research interests include calibration and validation of satellite-borne altimeter, synthesized aperture radar and scatterometer.
Email: wangcayun@mirslab.cn



Lin Mingsen was born in Fujian, China in 1963. He received Ph.D. degree from the Computing Center of Chinese Academy of Sciences in 1992. His research interests are microwave remote sensing of ocean wind, ocean satellite data processing algorithm and ground-based observations. He is a professor in the National Satellite Ocean Application Center.
Email: mslin@mail.nsoas.org.cn



Ma Chaofer was born in Hunan, China in 1971. He received Ph.D. degree from the Institute of Remote Sensing Applications, Chinese Academy of Sciences, Beijing, China in 2002, and mainly engaged in Cal/Val of China ocean satellites. He is responsible for the calibration and validation of the Haiyang Satellite. He is also the main participants of the Haiyang Satellite ground systems construction and on-orbit operation.
Email: mcf@mail.nsoas.org.cn



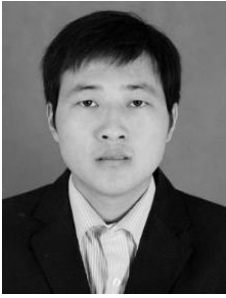
Dr. Xu is a professor with the National Microwave Remote Sensing Laboratory of CAS. His current technical interests are in areas of the space-borne radar altimeter design, synthetic aperture radar altimeter, and signal processing. He is the chief designer for the HY-2A/B/C satellite radar altimeter.
Email: xuke@mirslab.cn



Liu Peng was born in Hunan, China in 1983. He received the Ph.D. degree from the University of Chinese Academy of Sciences, Beijing, China, in 2018. He is a senior engineer in the National Space Science Center, CAS. His research interests include high-speed digital signal processing, FPGA programming, system integration and test.
Email: liupeng@mirslab.cn



Wang Te was born in Hunan, China in 1989. He received the M.D. degree from the Beijing University of Technology, China, in 2014. He works at the Nation Space Science Center, Chinese Academy of Sciences, Beijing. He is a senior engineer. He is engaged in the software development and data processing. He is one of the main participants in the HY-2B altimeter in-orbit calibration missions.
Email: wangte@mirslab.cn



Mu Bo was born in Shaanxi, China in 1985. He received the M.D. degree from the National Marine Environmental Forecasting Research Center, Beijing, China, in 2010. His main research field includes active microwave remote sensor calibration and validation, in-situ measurements technology and data applications. He is now the main participants of the HY-2A/B/C Satellite ground systems construction and on-orbit operation.

Email: mubo@mail.nsoas.org.cn



Zhu Jinbiao was born in Shandong, China in 1977. He received the M.D. degree from Tsinghua University, Beijing, China, in 2018. He is a professor of engineering, in Aerospace Information Research Institute, Chinese Academy of Sciences. He is engaged in the airborne remote sensing technologies and applications.

Email: zhujb@aircas.ac.cn



Guo Wei received Ph.D. degree in 1999, from the Institute of Electronics, Chinese Academy of Sciences. He did postdoctoral work in sea surface returned signal simulator (RSS) development for radar altimeter calibration at the National Space Science Center, CAS from 1999 to 2001. His research interests include calibration of HY-2 satellite altimeter by using reconstructive transponder. He is the primary investigator of the signal reconstructive transponder.

Email: guowei@mirslab.cn